Soil Biology and Biochemistry 197 (2024) 109503

Contents lists available at ScienceDirect

Soil Biology and Biochemistry

journal homepage: www.elsevier.com/locate/soilbio

Living and decaying roots as regulators of soil aggregation and organic matter formation—from the rhizosphere to the detritusphere

K. Witzgall [a,*], F.A. Steiner [a], B.D. Hesse [b,c], N. Riveras-Muñoz [d], V. Rodríguez [e], P.P.C. Teixeira [a], M. Li [g], R. Oses [h], O. Seguel [i], S. Seitz [d], D. Wagner [e,f], T. Scholten [d], F. Buegger [j], G. Angst [g,k,l], C.W. Mueller [a,m,n]

[a] Soil Science, TUM School of Life Sciences, Technical University of Munich, Freising-Weihenstephan, Germany
[b] Land Surface Atmosphere Interactions – AG Ecophysiology of Plants, TUM School of Life Sciences, Technical University of Munich, Freising-Weihenstephan, Germany
[c] Institute of Botany, Department of Integrative Biology and Biodiversity Research, University of Natural Resources and Life Sciences, Vienna, Austria
[d] Department of Geosciences, Soil Science and Geomorphology, University of Tübingen, Tübingen, Germany
[e] GFZ German Research Centre for Geosciences, Section Geomicrobiology, Potsdam, Germany
[f] Institute of Geosciences, University of Potsdam, Potsdam, Germany
[g] Biology Centre of the Czech Academy of Sciences, Institute of Soil Biology & SoWa Research Infrastructure, České Budějovice, Czech Republic
[h] Centro Regional de Investigación y Desarrollo Sustentable de Atacama (CRIDESAT), Universidad de Atacama, Copiapó, Chile
[i] Facultad de Ciencias Agronómicas, Universidad de Chile, Santiago, Chile
[j] Research Unit Environmental Simulation, Helmholtz Zentrum München (GmbH), German Research Center for Environmental Health, Neuherberg, Germany
[k] German Centre for Integrative Biodiversity Research Halle-Jena-Leipzig (iDiv), Leipzig, Germany
[l] Institute of Biology, Leipzig University, Leipzig, Germany
[m] Institute for Ecology, Chair of Soil Science, Technische Universitaet Berlin, Berlin, Germany
[n] Department of Geosciences and Natural Resource Management, University of Copenhagen, Copenhagen, Denmark

A B S T R A C T

In dryland ecosystems, typically characterized by sparse vegetation and nutrient scarcity, pioneer plants exert a critical role in the build-up of soil carbon (C). Continuous root-derived C inputs, including rhizodeposition and structural root litter, create hotspots of increased microbial activity and nutrient availability where biogeochemical processes, such as soil aggregation and the accumulation and stabilization of organic matter (OM), are promoted. Our study aims to disentangle the effects of root C inputs on soil aggregate formation, microbial community structures, and on the fate of OM—both before and after plant death, *i.e.,* during the transition from rhizosphere to detritusphere. This was realized in a two-phase incubation approach, tracing the natural and undisturbed transition from growth to subsequent decomposition of a pioneer plant-root system (*Helenium aromaticum*) in a semi-arid topsoil and subsoil. We quantified water-stable aggregates, investigated the fate and composition of OM separated into particulate and mineral-associated OM fractions (POM and MAOM), and observed successional changes in the root-associated microbiome. Our results underscore the significance of roots as vectors for macroaggregation within the rhizosphere in both topsoil and subsoil, associated with a particularly strong increase in fungal abundance in the subsoil. In topsoil, we identified root legacy effects in the detritusphere, as root-induced macroaggregation persisted after plant death, a phenomenon not observed in subsoil. These root legacy effects were accompanied by a clear succession towards gram + bacteria, which appeared to outcompete fungi during root decomposition. The increased availability of decaying litter surfaces further facilitated the protection of particulate OM via the occlusion into aggregates. Overall, to gain a holistic understanding of plant-microbe-soil interactions, we emphasize the need for more studies that span over the full temporal dimension from living to dying plants in intact soil systems.

1. Introduction

Global drylands cover nearly half of Earth's land surface, where water scarcity severely limits vegetation cover and plant production. In these hyper-arid, arid, or semiarid environments, soils are typically characterized by low nutrient and soil organic matter (OM) contents, high susceptibility to soil erosion and disturbance, and slow rates of soil formation and nutrient turnover (Chandler et al., 2019; Scholes, 2020). Despite these conditions, early colonizing primary producers, *i.e.,* pioneer plants and microorganisms, can establish where vegetation is otherwise sparse, and thereby have a fundamental role in the development and overall functionality of dryland soil ecosystems (Uroz et al., 2009; Esperschütz et al., 2011; Riveras-Muñoz et al., 2022). Here, the organic C provided by pioneering plants, *e.g.,* via root exudates or

* Corresponding author. Emil-Ramann-Str. 2, 85354, Freising, Germany.
E-mail address: kristina.witzgall@tum.de (K. Witzgall).

https://doi.org/10.1016/j.soilbio.2024.109503
Received 13 November 2023; Received in revised form 15 June 2024; Accepted 17 June 2024
Available online 18 June 2024

structural plant and root residues, marks the starting point for OM formation and build-up. The allocation of OM from plants to soil fundamentally shapes the soil environment, *e.g.,* by driving the formation of soil aggregate structures, improving habitat quality and versatility for the developing microbiome, providing nutrient sources for microbial and plant uptake, and for increasing water retention and water availability for plants (Denef et al., 2002; Murphy, 2015; Kravchenko and Guber, 2017; Bucka et al., 2019; Lal, 2020). Overall, this favors subsequent plant establishment and growth with implications for the continued development of the soil ecosystem.

A critical aspect of the plant-associated contribution to these soil processes occurs at the root-soil interface, *i.e.,* within the rhizosphere. As plants grow, their roots physically alter soil minerals, and root-associated microorganisms release weathering agents (*e.g.,* organic acids; Uroz et al., 2009) that mobilize essential soil nutrients (Gregory, 2022). In addition, the release of rhizodeposits at the root-soil interface represents a major pathway for the build-up of rather persistent mineral-associated OM (MAOM) in soil (Sokol et al., 2019; Villarino et al., 2021). Moreover, the increased abundance of labile C in the rhizosphere stimulates the growth and activity of microorganisms. This in turn drives the formation of aggregates via microbially derived binding agents (*i.e.,* extracellular polymeric substances; EPS) or via the enmeshment facilitated by fungal hyphae (Chenu and Consentino, 2011; Costa et al., 2018). In addition, root exudates (*e.g.,* root mucilage or polysaccharide exudates) can either adhere directly to mineral surfaces or function as glue-like binding agents, binding soil particles together, forming MAOM (Rötzer et al., 2023) and driving soil aggregation (Baumert et al., 2018). As such, roots substantially shape the chemical, physical, and biological nature of the soil at the root-soil interface, and the rhizosphere is widely recognized as a dynamic system in both space and time (Jones et al., 2009; Hinsinger et al., 2009; Kuzyakov and Razavi, 2019). However, relatively little is known about the temporal changes in processes occurring in the rhizosphere, as well as potential long-term effects of the living root system that may persist beyond the lifetime of the roots (Oliver et al., 2021). These effects, so-called "root legacy effects', might have implications for soil physical, chemical, and biological parameters that can remain in the soil after plant death and thus shape the subsequent detritusphere (Wurst and Ohgushi, 2015).

As the rhizosphere transitions to a root detritusphere and the release of root exudates ceases, the soil environment in the vicinity of the decaying root changes. In the early stages of the rhizosphere-detritusphere transition, the concentration of easily available and water-soluble compounds from the decaying root litter is still high (Cotrufo et al., 2015). In addition, the microbial community is influenced by the labile C inputs remaining from the rhizosphere, which is thought to accelerate the decomposition and transformation of root litter into soil OM (SOM) in the developing detritusphere (Wang et al., 2014). Over time, bioavailable compounds are gradually depleted and replaced by complex and slowly decomposing compounds. This has implications for the microbial community composition, driving a succession of microbial communities from microorganisms that rely on root exudates for energy to those involved in the decomposition of more recalcitrant litter compounds (Berg and McClaugherty, 2008; Theuerl and Buscot, 2010; Poll et al., 2010). This can be reflected in the composition of the bacterial community, as a common indicator of decreasing availability of labile C sources is the relative increase in gram positive (gram+) bacteria compared to gram negative (gram−) bacteria (Fanin et al., 2019). In the resulting detritusphere, the degradation of litter residues constitutes a hotspot for SOM formation, similar to the rhizosphere. This occurs by a variety of mechanisms, including the direct formation of MAOM achieved by the association of microbial-derived OM to mineral surfaces (Kopittke et al., 2020; Vidal et al., 2021), or via the occlusion of particulate OM (POM) within aggregates directly at the surface of decaying litter (Witzgall et al., 2021).

The rhizosphere and the detritusphere both represent hotspots for root-microbe-soil interactions, driving the formation of soil structures and the development and preservation of SOM—not only in the near-root environment, but also at larger scales (Richter et al., 2007). Similarly, these effects also extend from surface soils into the subsoil, where roots constitute a major—if not the only—source of C into the deeper soil horizons otherwise characterized by low OM contents, heterogeneously distributed C, and low microbial activity (Rasse et al., 2005; Chabbi et al., 2009). Previous studies demonstrate how the importance of root C inputs for OM formation (Angst et al., 2018), long-term C persistence (Eusterhues et al., 2003), and macroaggregation (Baumert et al., 2018) increase with increasing soil depth. In addition, Peixoto et al. (2020) show enhanced stabilization of root-derived C inputs in subsoils compared to in topsoil, and Wang et al. (2014) found increased incorporation rates of lignin-rich root derivatives into macroaggregates in subsoils. In semiarid shrub and grasslands, the deeper soil layers account for more than half of the total SOC stock across the soil profile (Jobbágy and Jackson, 2001), and the subsoil C stock is expected to be less vulnerable to changes in climate and land management compared to semiarid surface soils (Albaladejo et al., 2013). Despite the significance of roots as a primary C source, the fluxes and stabilization mechanisms of root C in subsoils remain unknown (Gregory, 2022), particularly so in the context of dryland ecosystems.

Here, we examine the interactions of root OM inputs with soil aggregate formation and the fate of SOM into POM and MAOM at the root-soil interface in living and decaying root systems of a semiarid top- and subsoil. In order to simulate these processes during the early stages of soil formation, two incubation phases were conducted, mimicking the natural growth process of a pioneer perennial herbaceous plant species (*Helenium aromaticum (Hook.) L. H. Bailey*); the first phase with living plants ('rhizosphere phase') with rhizodeposits as the main C input, followed by a decomposition phase ('detritusphere phase'), with plant and root litter as the main C input source (Fig. S1-Fig. S2). While numerous studies have contributed to our understanding of biogeochemical and microbial processes in both the rhizosphere and detritusphere (*e.g.,* Poll et al., 2008; Marschner et al., 2012; Tian et al., 2013; Vidal et al., 2021), these systems are often studied separately. This means that the succession from a living to a decaying root system is not included, nor are the potential legacy effects from the rhizosphere that could influence processes in the developing detritusphere (Wurst and Ohgushi, 2015). Furthermore, potential interactions between rhizodeposits and root litter as the two main root C inputs to SOM are unknown.

To address this research gap, we employed an experimental design in which the transition from rhizosphere to root detritusphere, as well as the establishment of the root-associated microbiome, remained undisturbed. Replicates were sampled at two time points, at the end of the rhizosphere and detritusphere phase, after which the distribution of water-stable aggregates and their contribution to the total C and N pool were quantified by wet-sieving. The fate and chemical composition (C, N, ^{13}C and ^{15}N) of OM in POM (free POM (fPOM), occluded POM (oPOM and $oPOM_{<20\mu m}$)) and MAOM was determined by density fractionation and ^{13}C CP-MAS NMR. Lignin-derived phenols were extracted from plant and root biomass, and the structure of root-associated microbial communities in the rhizosphere and detritusphere was characterized by phospholipid fatty acid (PLFA) extractions. We hypothesized that roots would promote the formation of water-stable macroaggregates in both topsoil and subsoil, and that root-induced aggregation would remain after plant death in the detritusphere as root legacy effects. We assumed that microbial abundance would increase in the rhizosphere, particularly in the C-poor subsoil, due to the increased abundance of labile C around the roots. We further hypothesized that the transition to the detritusphere, as labile C compounds are depleted and replaced by more complex litter-derived compounds, would induce a succession in the root-associated microbiome, specifically towards increasing gram + bacterial abundance.

2. Material and methods

2.1. Study site and soil sampling

Soil was sampled from five subplots on south-facing top slopes within the Santa Gracia Natural Reserve, located in the Coquimbo Region in Chile (29°44′26.3″S, 71°09′01.2″W) with mean annual precipitation of 89 mm yr^{-1} and mean annual air temperature of 13.7 °C (Ministerio de Obras Públicas, 2017). All five subplots were classified as Cambisol according to the WRB (IUSS Working Group WRB, 2015). Vegetation was dominated by shrubs (30–40% coverage; including *Proustia cuneifolia, Balbisia peduncularis, Cordia decandra* and *Baccharis paniculatum*), classified as 'Interior Mediterranean desert scrub' (Luebert and Pliscoff, 2006), and heavily disturbed by grazing animals (Oeser et al., 2018). The sampling site was selected as a suitable representation of an initial dryland soil with low vegetation cover, low organic C content, shallow and weakly structured A horizon (Bernhard et al., 2018). Topsoil and subsoil material was collected and sieved (<2 mm) from the profile walls of A and B horizons (0–3 cm and 5–30 cm, respectively), representing soils at different stages of development (Table S1). This allowed us to directly compare topsoil and subsoil, but also to use the subsoil as a model system for initial soil formation via plant-soil interactions in a saprolitic material.

2.2. Soil preparation and incubation setup

The topsoil and subsoil material from the five subplots was homogenized and cleared of plant residues and seeds to prevent unwanted germination during incubation. The two soil materials (topsoil and subsoil) were weighed separately into pots (350 cm^3) aiming to resemble bulk density according to field conditions (1.6–1.7 g cm^{-3}; Bernhard et al., 2018). Pre-germinated seeds (*Helenium aromaticum (Hook.) L. H. Bailey*) were sown on half of the pots, while the other half was left free of plants and hereafter referred to as controls (Fig. S1). After the initial incubation period of 70 days under greenhouse conditions ('rhizosphere phase'), half of the samples were harvested, while the remaining half were placed in complete darkness and incubated at room temperature for 100 days ('detritusphere phase'). The samples were left completely undisturbed during decomposition, meaning that aboveground biomass was left to decompose on the soil surface. During both incubation phases, the samples received 6 mL of rainwater per day, without correcting for potential differences in soil moisture, *e.g.* due to differences in plant water use between treatments.

After incubation, the plants were cut just above the soil surface and the roots were separated from the bulk soil (Fig. S2). To minimize artifact effects of biocrust on the soil surface, the top 0–1 cm of all samples was discarded (Weber et al., 2022). The soil sticking to the roots was collected separately and hereafter referred to as 'root-adhering soil'. Since the pots were thoroughly rooted, the remaining soil in the pots was defined as 'rhizosphere soil'. During the detritusphere phase, there was not enough soil adhering to the decaying roots to sample separately, meaning that all the soil in the pots were collected as 'detritusphere soil' from this phase. After incubation, replicate samples were combined in pairs (two by two) to form composite replicates. As such, there were initially 12 replicates per treatment during the incubation phases (48 pots in total), which later resulted in 6 composite replicates for each treatment for subsequent analyses. After harvest, plant and root samples were immediately frozen in liquid N. A homogenized aliquot of each soil sample was freeze-dried and stored at −20 °C for later microbial analyses (section 2.3). The remaining bulk soil material was air-dried at room temperature. Plant and root samples were analyzed for C, N, ^{13}C, ^{15}N (section 2.6), and lignin-derived phenols were extracted (section 2.8). Basic soil parameters (pH and electrical conductivity) were determined for soil material before and after each incubation period, and the gravimetric water content was determined for incubated samples (Table S1).

2.3. Phospholipid fatty acid analyses

Phospholipid fatty acid (PLFA) patterns were recorded as reported by Frostegård et al. (1993) with adjustments according to the modified method by Kramer et al. (2013). Briefly, 4 g topsoil and 12 g subsoil were vortexed with Bligh & Dyer solution [methanol, chloroform, citrate buffer (pH = 4 ± 0.1), 2:1:0.8, v/v/v] to extract lipids from the soil. Phospholipids were separated from neutral lipids and glycolipids by solid phase extraction on silica tubes (0.5 g SiOH, Bond Elut SI, Agilent Technologies) and later evaporated at 40 °C under a stream of N_2 (~100 bar). The separated PLFAs were turned into fatty acid methyl esters (FAMEs) via alkaline methanolysis and later resolved in isooctane, from which the concentration of FAMEs was quantified via gas chromatography coupled to a flame ionization detector (Thermo Scientific Trace 1310, Waltham, MA, USA). The gas chromatograph was equipped with a ZB-5HT fused silica capillary column (60 m, 0.25 I.D., 0.25 μm film thickness; Zebron Capillary GC column, Inforno™). The following FAMEs were selected for quantification; bacteria: C15:0 and C17:0, including gram + bacteria: i15:0, a15:0, i16:0 and i17:0 (O'Leary and Wilkinson, 1988) and gram− bacteria: 16:1ω7, cy17:0 and cy19:0 (Phillips et al., 2002), fungi: 18:2ω6 and 18:1ω9 and unspecified microorganisms: C14:0, C16:0, 18:1ω7, C18:0 and C20:0. These markers were used to calculate fungi to bacteria (fungi:bacteria) and gram+: gram− ratios. The quantification and classification of PLFAs were based on non-adecanoic acid methyl ester (19:0) as the internal standard.

2.4. Aggregate fractionation

To separate water-stable aggregates, 5 g air-dried aliquots of bulk soil were rewetted with deionized water for 30 min and placed on a sieve tower (mesh size: 250 and 53 μm, diameter: 100 mm) in a beaker containing 2 L deionized water. Aggregates were separated into macroaggregates (2000-250 μm), large microaggregates (250-53 μm) and small microaggregates including silt and clay particles (<53 μm) by gentle up and downward movement (2 cm) repeated for 130 cycles, while the soil material was completely submerged in water (Baumert et al., 2018). The small microaggregate fraction was retained on a 0.45-μm filter, and all samples were finally dried at 40 °C. On average, 99.3 ± 0.4% of the soil material was recovered from the fractionation process.

2.5. Density and particle size fractionation

Bulk soil was separated into five distinct OM fractions using a combined density and particle size fractionation approach according to Mueller and Koegel-Knabner (2009). Briefly, 30 g of air-dried soil (50 g for subsoil) was saturated with a polytungstate solution ($Na_6[H_2W_{12}O_{40}]$) at a density of 1.8 g cm^{-3} for 12 h, after which free-floating particulate OM (fPOM) was separated from the bulk using a vacuum pump. Ultrasonic dispersion (Bandelin, Sonoplus HD 2200; 440 J mL^{-1}) was used to release occluded POM (oPOM) from aggregated soil structures, and the fraction was later sieved at 20 μm to yield oPOM and oPOM <20 μm ($oPOM_{small}$). Finally, the remaining mineral material was separated into two mineral fractions: $MAOM_{>63\mu m}$ and $MAOM_{<63\mu m}$. All fractions were washed with deionized water, pressure filtered (0.22 μm) below an electrical conductivity of <5 μS cm^{-1}, ground and freeze-dried before elemental analysis.

2.6. Carbon and nitrogen measurements of bulk soil and fractions

Plant and root biomass, root-adhering soil, and OM fractions were analyzed for C, N, ^{13}C, and ^{15}N (Delta V Advantage, Thermo Fisher, Dreieich, Germany) coupled with an elemental analyzer (Euro EA, Eurovector, Milano, Italy). The aggregate size fractions were analyzed for C and N (EuroVector EuroEA3000 Elemental Analyzer). The presence of $CaCO_3$ was examined through gas volumetric analysis (Scheibler Calcimeter; Eijkelkamp, Giesbeek, Netherlands) in which HCl was added

to the soil and the gas pressure of the resulting CO_2 was used to calculate $CaCO_3$ contents. No reaction could be determined and the presence of $CaCO_3$ could thereby be ruled out, meaning that total C contents were considered equal to total OC contents.

2.7. ^{13}C nuclear magnetic resonance spectroscopy

The chemical composition of below- and aboveground plant material and POM fractions was determined via solid state ^{13}C CP-MAS NMR spectroscopy (Bruker DSX 200, Bruker BioSpin GmbH, Karlsruhe, Germany). The samples, placed in 7-mm zirconium dioxide rotors, were spun at 6.8 kHz with an acquisition time of 0.01024 s and a delay time of 1.0 s for plant material and 0.4 s for POM fractions. After a manual baseline correction, the recorded ^{13}C spectra were quantified according to Mueller and Koegel-Knabner (2009) with the following chemical shift regions: alkyl C (−10–45 ppm), O alkyl C (45–110 ppm), aromatic C (110–160 ppm), and carbonyl/carboxyl C (160–220 ppm). Further, we computed the alkyl C/O alkyl C ratio (−10-45/45-110 ppm) according to Baldock et al. (1997) as well as the O alkyl C/methoxyl C and N alkyl C ratio (70–75/52-57 ppm) according to Bonanomi et al. (2013) as a proxy for the stage of decomposition. Lastly, the spectra were modeled via the molecular mixing model (Nelson and Baldock, 2005; Prater et al., 2020) to compute the relative contribution of carbohydrates, proteins, lignins, lipids, and carbonyls. For the model, the chemical shift regions 0–45, 45–60, 60–95, 95–110, 100–145, 145–165, and 165–215 ppm were applied.

2.8. Lignin extraction

Lignin-derived phenols were extracted from plant and root samples via cupric oxide (CuO) oxidation according to Angst et al. (2017). Samples containing at least 5 mg C were weighed into pressure digestion vessels with 50 mg ammonium iron (II) sulfate hexahydrate and 300 mg CuO, saturated with 2 M NaOH and shaken at 155 °C for 3 h. The NaOH was separated by centrifugation and acidified with 6 M HCl, and the remaining solution was extracted with ethyl acetate, filtered over Na_2SO_4, and dried under N_2. The sum of vanillyl, syringyl, and cinnamyl units (VSC) was used as an indicator for total lignin contents. The ratio between lignin-derived phenolic acids and their corresponding aldehydes was computed for vanillyl ($(Ac/Al)_V$) as well as combined for all units (Ac/Al).

2.9. Statistics

We tested all parameters for homoscedasticity using Levene's test and the residuals of each model were tested for Normality using QQ-

Table 1
Elemental and isotopic composition of above- and belowround biomass. Relative amounts of carbohydrates, proteins, lignin, lipids, and carbonyls (derived from a molecular mixing model) and lignin monomers in above- and belowground biomass, from two incubation phases; with living plants ('rhizosphere phase') and decaying plants ('detritusphere phase'). The plants were growing in topsoil and subsoil. Values represent means of n = 6 for all samples except for decaying plants (n = 2) and roots (n = 1) in subsoils. Asterisks denote significant differences between the two incubation phases ($^{\bullet}P < 0.1$, $^{*}P < 0.05$, $^{**}P < 0.01$ and $^{***}P < 0.001$).

		Topsoil				Subsoil			
		Rhizosphere phase		Detritusphere phase		Rhizosphere phase		Detritusphere phase	
		Aboveground	Belowground	Aboveground	Belowground	Aboveground	Belowground	Aboveground	Belowground
Basic properties	C (mg g^{-1})	4.06 ± 0.20	3.70 ± 0.08	3.49 ± 0.47	3.97 ± 0.74	3.16 ± 0.50	3.70 ± 0.09	3.23 ±*n.a.*	3.36 ± 1.43
	N (mg g^{-1})	0.17 ± 0.05**	0.11 ± 0.02	0.25 ± 0.06**	0.11 ± 0.02	0.09 ± 0.01	0.07 ± 0.00	0.11 ±*n.a.*	0.10 ± 0.04
	C:N	25.61 ± 7.77**	34.43 ± 6.69	14.67 ± 3.43**	37.26 ± 8.89	33.58 ± 2.90	53.54 ± 3.99***	28.70 ±*n.a.*	32.37 ± 5.27***
	Biomass (g)	0.47 ± 0.17***	0.44 ± 0.13***	0.11 ± 0.07***	0.03 ± 0.02***	0.25 ± 0.09	0.29 ± 0.03***	4 ±*n.a.*	0.02 ± 0.00***
	Total biomass (g)	0.90 ± 0.22***		0.13 ± 0.09***		0.54 ± 0.11***		0.05 ± 0.07***	
	Root:shoot	1.07 ± 0.48**		0.32 ± 0.20**		1.27 ± 0.37		0.24 ±*n.a.*	
	C (mg)	1.91 ± 0.78***	1.62 ± 0.51***	0.38 ± 0.29***	0.12 ± 0.09***	0.75 ± 0.21	1.07 ± 0.12***	0.36 ±*n.a.*	0.06 ± 0.04***
	N (mg)	0.07 ± 0.02***	0.05 ± 0.01***	0.03 ± 0.02***	0.00 ± 0.01***	0.02 ± 0.01	0.02 ± 0.00	0.01 ±*n.a.*	0.00 ± 0.00
	$\delta^{15}N$ (‰ air N_2)	4.96 ± 0.78	4.14 ± 0.59$^{\bullet}$	4.29 ± 0.71	3.22 ± 0.81$^{\bullet}$	4.66 ± 0.61	4.41 ± 0.45***	3.94 ±*n.a.*	1.56 ± 0.53***
	$\delta^{13}C$ (‰ V-PDB)	−29.84 ± 0.78	−28.68 ± 0.51	−29.46 ± 1.34	−29.50 ± 1.01	−31.94 ± 0.39	−30.52 ± 0.35	−31.22 ±*n.a.*	−31.66 ± 1.76
Rel. Contents from mixing model (%)	$Carbohydrate_{NMR}$	53.68 ± 7.07$^{\bullet}$	57.69 ± 2.31**	42.67 ± 8.17$^{\bullet}$	44.60 ± 8.41**	47.38 ± 4.89	63.13 ± 5.09	49.78 ±*n.a.*	37.17 ±*n.a.*
	$Protein_{NMR}$	10.76 ± 3.47**	7.46 ± 1.36	19.81 ± 6.16**	7.39 ± 2.22	7.48 ± 0.69	4.57 ± 0.35	9.36 ±*n.a.*	7.39 ±*n.a.*
	$Lignin_{NMR}$	21.05 ± 2.04	22.30 ± 0.96***	25.10 ± 4.79	37.11 ± 4.57***	25.52 ± 2.46	20.54 ± 1.93	25.62 ±*n.a.*	42.83 ±*n.a.*
	$Lipid_{NMR}$	8.04 ± 1.28	5.93 ± 0.89	9.37 ± 1.85	3.42 ± 0.89	7.97 ± 0.92	4.63 ± 0.90	8.76 ±*n.a.*	1.66 ±*n.a.*
	$Carbonyl_{NMR}$	6.46 ± 2.99	6.62 ± 0.98**	3.04 ± 2.41	7.49 ± 3.01**	11.66 ± 2.18	7.13 ± 2.16	6.48 ±*n.a.*	10.94 ±*n.a.*
	$Lignin_{NMR}$:N	132.24 ± 34.21	207.66 ± 36.13$^{\bullet}$	106.31 ± 31.66	351.58 ± 80.547$^{\bullet}$	275.88 ± 41.97	295.67 ± 14.96	236.74 ±*n.a.*	428.00 ±*n.a.*
Lignin monomers	VSC (mg g^{-1} C)	58.89 ± 32.17	121.03 ± 47.54	51.96 ± 20.66	205.80 ± 81.72	39.37 ± 10.21	89.12 ± 40.70	40.41 ±*n.a.*	n.a. ±*n.a.*
	S:V	0.44 ± 0.10	0.66 ± 0.12**	0.42 ± 0.19	1.56 ± 0.41**	0.29 ± 0.06	0.77 ± 0.30	0.42 ±*n.a.*	n.a. ±*n.a.*
	C:V	0.19 ± 0.06	0.24 ± 0.03***	0.24 ± 0.14	0.09 ± 0.01***	0.20 ± 0.14	0.18 ± 0.12	0.26 ±*n.a.*	n.a. ±*n.a.*
	Ac:Al	0.34 ± 0.08	0.32 ± 0.03*	0.50 ± 0.23	0.55 ± 0.04*	0.39 ± 0.27	0.22 ± 0.15	0.48 ±*n.a.*	n.a. ±*n.a.*
	$Ac:Al_V$	0.11 ± 0.03	0.10 ± 0.02***	0.18 ± 0.04	0.87 ± 0.23***	0.11 ± 0.07	0.07 ± 0.03	0.15 ±*n.a.*	n.a. ±*n.a.*

Plots and the Shapiro-Wilk test. In cases where the assumption of normality or homoscedasticity was not met, the data was appropriately transformed. To evaluate differences between the data presented in Table 1, we conducted a one-way analysis of variance (ANOVA) with Tukey's honestly significant differences (HSD) as a post-hoc test. The remaining data was analyzed using mixed-effect models (package: nlme) using soil material (topsoil vs subsoil) and phase (rhizosphere phase vs detritusphere phase) as fixed factors and the ID as a random effect. All statistical testing was conducted in R (version 4.2.1; R Development Core Team, 2008) using RStudio (Version, 2022.07.2, R Core Team, Vienna, Austria; RStudio Team, 2015). Further, data shown in text and tables are given as the mean values and standard deviations.

3. Results

3.1. Growth and decomposition patterns of above- and belowground biomass

The soil material clearly impacted the growth of the above- (plant) and belowground (root) biomass, with lower plant and root biomass and lower C and N contents in the subsoil compared to the topsoil (Table 1). The soil material also influenced the elemental composition of belowground biomass, with broader C:N ratios in roots growing in the subsoil (54.54 ± 3.99) compared to the topsoil (34.43 ± 6.69; $P < 0.001$). The difference in root litter quality between the growing materials was further underlined by the higher $lignin_{NMR}$:N ratio (295.67 ± 14.96 in subsoil compared to 207.66 ± 36.13 in topsoil; $P = 0.001$). The decomposition of aboveground biomass was more progressed compared to belowground biomass, with approximately 7% of the biomass remaining after the detritusphere phase in both soil materials (compared to ~22% and 13% of roots remaining in topsoil and subsoil, respectively; Table 1).

The molecular mixing model according to Nelson and Baldock (2005) showed how the composition of both above- and belowground biomass changed with decomposition, with the concentration of $lignin_{NMR}$ increasing from 22.30 ± 0.96 to 37.11 ± 4.57% in decomposing roots in the topsoil ($P < 0.001$; Table 1). This was accompanied by a slight decrease in $carbohydrate_{NMR}$ (from 57.59 ± 2.31 to 44.60 ± 8.41%; $P = 0.008$). These patterns differed from the aboveground biomass, where instead the relative $protein_{NMR}$ content almost doubled with decomposition ($P = 0.004$), while the lignin content remained unaffected. The chemical composition of the decaying biomass in the subsoil could not be determined due to insufficient sample material remaining after decomposition.

The increased $lignin_{NMR}$ in decaying root biomass in the topsoil was corroborated by a slight, however not significant, increase in lignin monomers (from 121.03 ± 47.54 in living roots to 205.80 ± 81.72 mg VSC g^{-1} C in decaying roots; $P = 0.24$). The progressed decomposition of the roots in the topsoil was reflected in an increased Ac/Al_V ratio (from 0.10 ± 0.02 to 0.87 ± 0.23; Kögel-Knabner et al., 1988) and overall, in changed lignin composition as indicated by the changing S:V, C:V and Ac:Al ratios. This was not reflected in the aboveground biomass (Table 1).

3.2. Elemental and isotopic composition of rhizosphere and detritusphere soil

The introduction of a pioneer plant to the system did not notably change the elemental composition of the soil, neither in the rhizosphere phase nor in the detritusphere phase, with no significant changes in C and N content or in the C:N ratio compared to the controls (Fig. S3; Table S2). Overall, C and N decreased and C:N ratios narrowed over the course of the incubation with no clear distinction between planted and control samples (Fig. S3).

Stable isotope measurements only showed minor shifts in the natural abundance of ^{15}N and ^{13}C in root-adhering subsoil, which was slightly enriched in ^{15}N ($P = 0.011$) and depleted in ^{13}C ($P = 0.006$) compared to the bare soil controls (Fig. S4). The decrease in $\delta^{13}C$ was also weakly reflected in the topsoil ($P = 0.065$). Overall, the two soil materials differed strongly in their isotopic composition, with the subsoil enriched in ^{13}C but depleted in ^{15}N compared to the topsoil (Fig. S4).

3.3. Size and elemental distribution of water-stable aggregates

The living roots fostered the formation of macroaggregates in the topsoil, which was reflected in an increased mass contribution of the 2000-250 μm aggregate size obtained by submerged sieving (71.18 ± 3.90% compared to 64.38 ± 1.67% in controls, $P = 0.001$; Fig. S5). This was associated with lower mass contributions of the smaller aggregate size classes compared to controls ($P < 0.001$ for large microaggregates and $P = 0.081$ for small microaggregates). These patterns were only weakly reciprocated in the subsoil. Similarly, while the patterns persisted into the detritusphere incubation phase, the differences were no longer significant.

Root-induced aggregate formation was further emphasized by elevated organic C and N contents within the larger macroaggregates in the rhizosphere, *e.g.,* from 5.09 to 5.80 mg C g^{-1} fraction in topsoil ($P = 0.026$) and from 1.35 to 1.76 in subsoil ($P = 0.014$; Fig. 1 a and b). The C and N contribution of the fractions per g soil further emphasized the distinction of the larger macroaggregates, with higher contents of C and N (mg g^{-1} soil) in both topsoil and subsoil (Fig. c and d).

Interestingly, contrary to the topsoil, the root effect was not isolated to macroaggregates in the subsoil, but also resulted in elevated C and N contents in larger microaggregates (250-53 μm) compared to the corresponding controls (5.49 in rooted samples and 4.84 mg C g^{-1} soil in controls). In the topsoil, the effects of the living roots extended into the detritusphere phase in larger macroaggregates, with elevated C (5.99 in rooted compared to 5.27 C g^{-1} in controls, $P = 0.041$) and N (0.52 in rooted compared to 0.45 N g^{-1} in controls, $P = 0.060$; Fig. 1 c and d). This was not reflected in the subsoil.

3.4. Elemental distribution in specific organic matter fractions

Across treatments, the elemental compositions of the separated POM and MAOM fractions remained largely consistent, with almost no notable changes in their C and N contents around living or decaying roots (Fig. S6; Fig. S8). However, a clear change in the content of C and N (in mg g^{-1} soil) was observed in the $oPOM_{<20\mu m}$ fraction within the topsoil (Fig. 2 a and b). In the rhizosphere, the C content in $oPOM_{<20\mu m}$ decreased slightly compared to unplanted controls (from 1.37 to 0.95 mg C g^{-1} soil; $P = 0.089$). In the detritusphere, however, C in $oPOM_{<20\mu m}$ was preserved around decaying roots compared to decreasing C contents of the same fractions in controls (1.27 compared to 0.81; $P = 0.025$; Fig. 2 a and b). This was also reflected in the total amount of C allocated in $oPOM_{<20\mu m}$ in the detritusphere (38.07 compared to 24.44 mg C in controls; $P = 0.052$; Fig. S6) and further emphasized by the maintained relative C and N contribution of the fraction around decaying roots in topsoil (Fig. 2 c and d). This pattern was reversed around the living roots; although not significant, the total amount of C in $oPOM_{<20\mu m}$ was slightly lower compared to the controls (28.66 compared to 41.30 mg C; $P = 0.187$).

The changes in the $oPOM_{<20\mu m}$ fractions were not observed in the subsoil. Instead, there was a slight (non-significant) increase in the C contribution of the fPOM fraction in the subsoil rhizosphere (from 3.63 ± 0.74 to 6.59 ± 0.27%; $P = 0.154$; Fig. 2 c). This led to increased C:N ratios of the fPOM fractions around living but also around decaying roots, from 24.37 to 26.88 in the rhizosphere ($P = 0.053$) and from 22.91 to 25.36 in the detritusphere ($P = 0.086$, Fig. S6).

Although not significant, the fPOM fraction in the subsoil rhizosphere was further depleted in ^{15}N (from 4.44 in controls to 4.00‰ in rooted samples; $P < 0.001$). In the detritusphere, this pattern was reversed, with the fraction instead enriched in ^{15}N (from 4.26 in controls

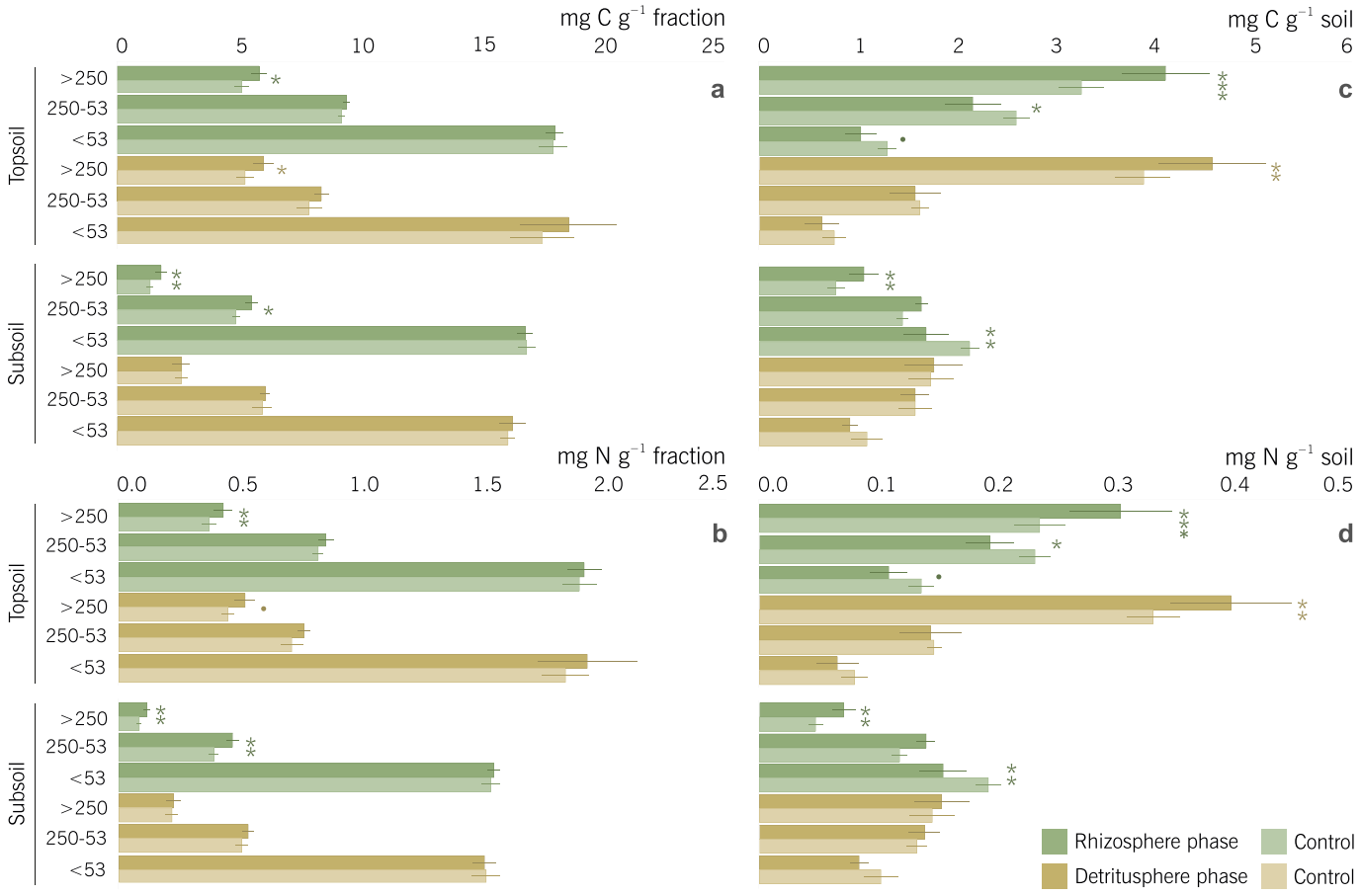

Fig. 1. C and N contents in water-stable aggregate size classes. The contents of **a** C and **b** N (in mg g^{-1} fraction) in three water-stable aggregate-size classes and the concentrations of **c** C and **d** N (in mg g^{-1} soil) in the bulk soil. Green represents a living root phase (rhizosphere) and brown a decaying root phase (detritusphere) together with corresponding controls. Asterisks denote significant differences between rooted and control samples ($^{\bullet}P < 0.1$, $^{*}P < 0.05$, $^{**}P < 0.01$, $^{***}P < 0.001$). Bars represent means ± SD (n = 6 independent replicates).

to 4.77‰ in rooted samples; $P < 0.001$; Fig. S7). In MAOM fractions, we did not determine any significant changes in the isotopic composition across treatments (Fig. S9). The chemical composition of the separated POM fractions (determined via ^{13}C CP-MAS NMR) showed no differences between treatments, with little to no effect of the living or decaying roots. Further, the integrated regions showed similar chemical composition of the fractions, not only between the incubation phases, but also between the substrates (Table S3).

3.5. Phospholipid fatty acid analysis

Microbially derived FAs increased in the rhizosphere of the topsoil substrate (from 24.62 to 32.66 nmol C-FA g^{-1} soil; $P = 0.005$) into the detritusphere phase, with the elevated microbial abundance being maintained in rooted topsoil samples compared to controls (29.64 versus 20.00 nmol C-FA g^{-1} soil; $P = 0.002$; Fig. 3 a). Around living roots, both fungi and bacteria increased uniformly in the topsoil (Fig. 3 b and c), as reflected by the fungi:bacteria ratio, which remained similar to controls despite the overall increase in FAs (Fig. 3 d). However, as decomposition progressed, the fungal abundance around decaying roots decreased, while bacterial abundance was maintained. This was associated with a relative increase in gram + bacteria around the decaying roots, as reflected in the elevated gram+:gram− ratio (from 0.70 to 0.90; $P = 0.009$; Fig. 3 e). In the subsoil, fungal abundance increased significantly around living roots compared to controls ($P = 0.007$), similar to the differences observed in topsoil, with a shift in the fungi:bacteria ratio from 0.58 to 0.75 ($P = 0.005$). During the detritusphere phase, no difference between roots and controls was observed in the subsoil.

4. Discussion

The purpose of this study was to investigate how plant roots drive soil structure formation and SOM build-up during early stages of soil development in a dryland soil system. The experiment was designed to follow the natural undisturbed succession from rhizosphere to detritusphere, aiming at capturing possible legacy effects from the rhizosphere influencing the development of the detritusphere. This allowed for the direct observation of changes in SOM formation, aggregation, and microbial community composition during phases where C inputs were primarily derived from either active rhizodeposition ('rhizosphere phase') or decaying root litter inputs ('detritusphere phase'). We hereby demonstrate how root-microbe-soil interactions change during the transition from rhizosphere to detritusphere, and how these processes are partially constrained—or counterbalanced—depending on the soil substrate in which the roots grow and later decompose.

4.1. The rhizosphere: rhizodeposition as C input

In the studied dryland soil, roots induced a shift in soil aggregation in the rhizosphere, leading to an increased contribution of water-stable macroaggregates to the total mass and an increased allocation of C and N to macroaggregates in both topsoil and subsoil (Fig. S5; Fig. 1 c and d; Fig. 4 a). This root effect is consistent with the well-established consensus that plant roots drive the formation of coarser aggregate structures, for example via root-derived gluing agents or direct entanglement of soil particles (Tisdall and Oades 1982; Six et al., 2004; Angst et al., 2018; Gregory, 2022).

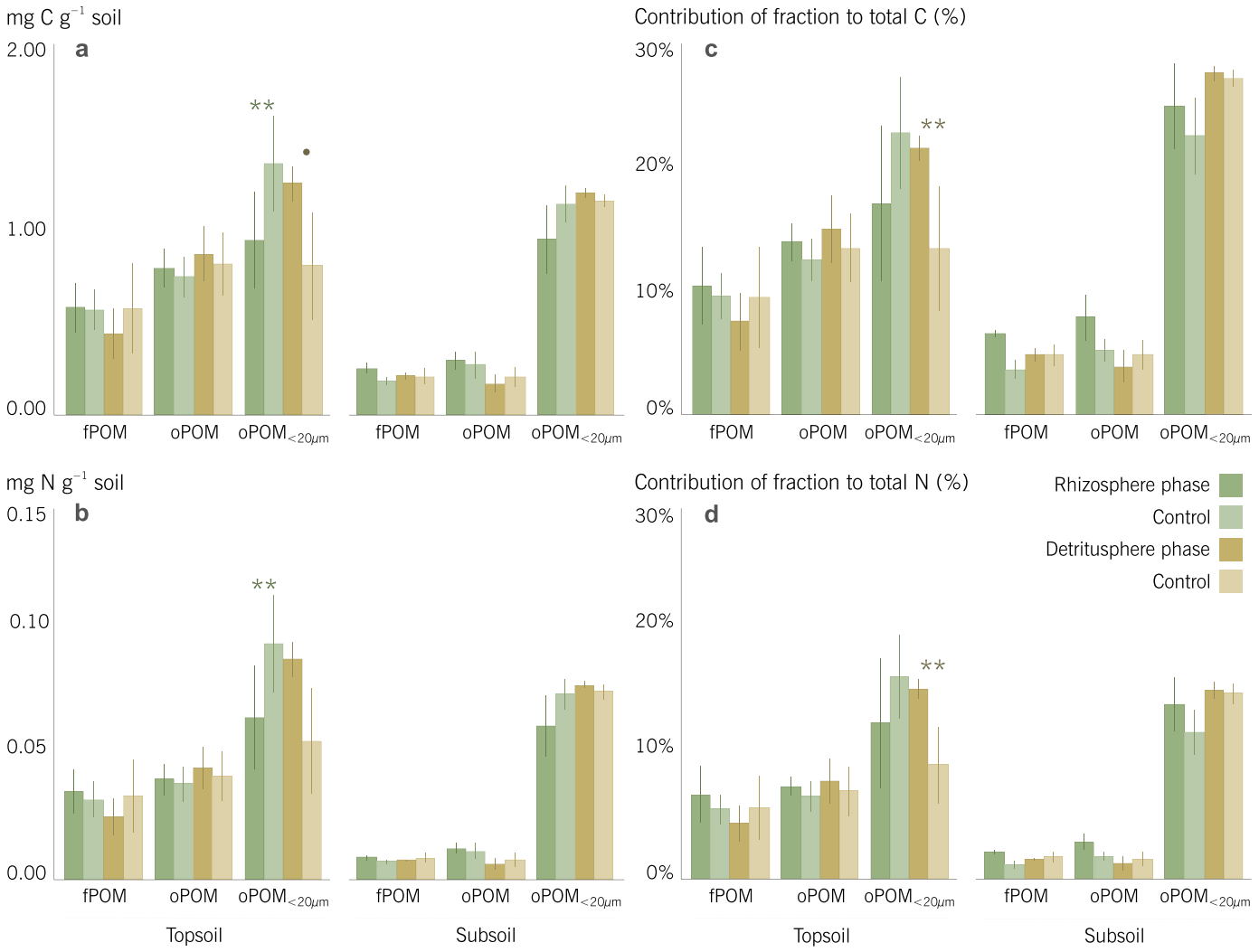

Fig. 2. C and N contents in and contributions of particulate organic matter fractions. The content of **a** C and **b** N (in mg g^{-1} soil) and the contribution of **c** C and **d** N to the total stock (in %) of organic matter fractions (fPOM, oPOM and oPOM$_{<20\mu m}$). Green represents a living root phase (rhizosphere) and brown a decaying root phase (detritusphere) together with corresponding controls in faded colors. Asterisks denote significant differences between rooted and control samples ($^{\bullet}P < 0.1$, $^{*}P < 0.05$, $^{**}P < 0.01$, $^{***}P < 0.001$). Bars represent means ± SD (n = 3 independent replicates).

The pioneer plant shaped the composition of the microbial community around the living roots. Driven by the easily available OM from the rhizodeposits, the total microbial abundance increased significantly in the topsoil rhizosphere (Fig. 3 a). Interestingly, both fungi and bacteria increased similarly (Fig. 3 b and c), meaning that the overall community structure remained unaffected by rooting (Fig. 4 c). In contrast, there was no substantial increase in total microbial abundance in the subsoil rhizosphere. Instead, we determine a pronounced community shift towards a higher relative abundance of fungi in the subsoil (Fig. 3 b), while bacterial abundance remained unaffected by the roots (Fig. 4 b). These findings are in accordance with the widely accepted notion that conditions in the rhizosphere favor fungi over other microbial groups (Butler et al., 2003; Brant et al., 2006; Denef et al., 2009). This could be due to the lower content and diversity of SOM (including native OM) in the subsoil, where the filamentous growth of the fungal mycelium benefit fungi in gaining access to heterogeneously distributed OM resources, compared to bacteria with rather restricted motility in the soil (De Boer et al., 2005).

Roots grown in the subsoil were of lower litter quality (higher lignin$_{NMR}$:N ratio) compared to in the topsoil, and as fungi are adapted to assimilate more complex C resources from litter, this may have further amplified the distinction of fungi in the subsoil (Poll et al., 2006). Moreover, it is possible that this shift towards increased fungal dominance in the subsoil contributes not only to root-induced macroaggregation, but also to the observed microaggregation in the subsoil rhizosphere, which was not observed in the topsoil (Fig. 1 a and b). Fungal hyphae as vectors for macroaggregation have been widely reported (*e.g.,* Bossuyt et al., 2001; Lehmann et al., 2020; Bucka et al., 2021), but evidence for the processes associated with fungal-induced microaggregation remains scarce. Vidal et al. (2018) show how hyphae are in fact closely linked to soil microstructure formation directly at the root-soil interface. Rillig and Mummey (2006) further point to mycorrhizal fungal mycelial products as drivers of the formation of smaller aggregates. As arbuscular mycorrhizal colonization has been reported for the pioneer species used in this study growing in adjacent study sites (*Helenium aromaticum*; Dhillion et al., 1995), mycelial byproducts and mutualistic plant-microbial interactions may be a contributing factor to the increased microaggregation in the subsoil. The increased fungal abundance in the subsoil rhizosphere is consistent with the findings of Baumert et al. (2021) and overall emphasizes fungi as key players in the assimilation of root-derived C compounds in the subsoil. In association with the increased fungal dominance in the subsoil rhizosphere, we determine that the effect of the roots on aggregation was not isolated to macroaggregates in the subsoil but extended to larger

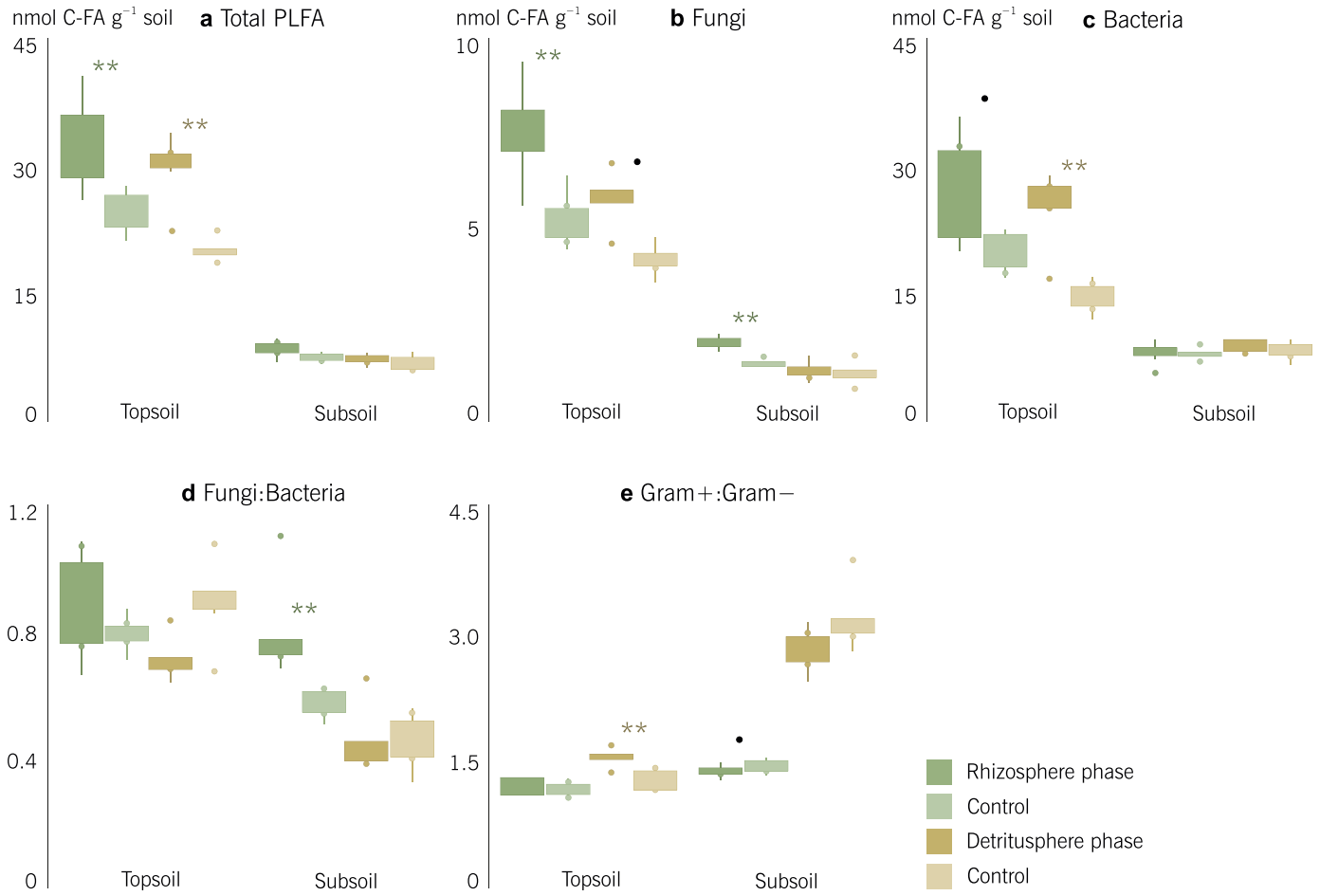

Fig. 3. PLFA profiling of microbial community structure. The **a** total content of extracted fatty acids (in nmol C-FA g^{-1}), the content of markers associated with **b** fungi (nmol C-FA g^{-1}) and **c** bacteria (nmol C-FA g^{-1}) and the **d** fungi:bacteria ratio and **e** gram+:gram− ratio in a topsoil and subsoil. Green boxes represent the living root phase (rhizosphere) and brown the decaying root phase (detritusphere) together with corresponding controls in faded colors. Asterisks denote significant differences between rooted and control samples ($^{\bullet}P < 0.1$, $^{*}P < 0.05$, $^{**}P < 0.01$, $^{***}P < 0.001$). Box plots indicate medians (line) and means (x), where the first (Q1) and third (Q3) quartile are represented by the lower, respectively upper bounds of the box. Error bars represent the data range, bounded to 1.5 × (Q3-Q1; n = 6 independent replicates).

microaggregates, where C and N contents were elevated compared to the controls (Fig. 1 a and b), which further highlights the importance of labile root-derived gluing agents for aggregate formation during early rhizosphere development in C poor subsoils (Baumert et al., 2018).

4.2. *The detritusphere: root litter as C input*

After plant death, as the rhizosphere transitioned to a detritusphere, the initially formed root-induced macroaggregation remained in the topsoil but entirely disintegrated in the subsoil. The overall lack of aggregate stability over time is consistent with observations showing that a continuous input of OM is necessary to maintain aggregate structures, and that the disintegration of macroaggregates begins during early stages of decomposition when available C sources and microbial activity decline (*e.g.,* Golchin et al., 1997; Helfrich et al., 2008). In the present study, disintegration of newly formed aggregates was indeed particularly pronounced in the C poor subsoil (Fig. 4 f), which is supported by the work of Bucka et al. (2021), who report low mechanical stability of newly formed macroaggregates after OM addition in initial soils compared to greater retained aggregate stability in mature soils (Felde et al., 2020). This suggests that aggregates initially formed in the rhizosphere are only loosely connected, and that a living root system—or continuous C input—is a prerequisite for aggregate formation and persistence in soil systems with otherwise limited C inputs. Furthermore, these results suggest that a certain 'backbone' of native C, as in the topsoil, is required for long-term aggregate stabilization in arid soil systems. The difference between topsoil and subsoil may have been further amplified by the fact that roots grown in subsoil had lower litter quality (higher C:N and $\text{lignin}_{\text{NMR}}$:N ratio; Table 1; Walela et al., 2014) compared to those grown in topsoil, further reinforcing the limiting conditions for microbial activity.

The transition from a living to a decaying root system, and thereby from C inputs dominated by low molecular weight compounds to more complex structural litter-derived C sources, shaped the composition and structure of the microbial community. The relative dominance of gram+ over gram− bacteria increased distinctively in the detritusphere of both soil substrates (Fig. 3 e). This was likely driven by the increasing complexity of the litter resources as the decomposition progressed (*e.g.,* as indicated by increasing Ac/Al_{V} ratios; Table 1), favoring gram+ bacteria which are specialized in the processing of complex C sources (Fanin et al., 2019; Denef et al., 2009; Butler et al., 2003). This is supported by Shi et al., (2018), who show how the microbial genetic potential to decompose complex macromolecular compounds increases in the absence of living roots, while root exudates in the rhizosphere instead promote the development of a microbial community with increased capacity to utilize low molecular weight compounds. This underscores how the presence of living and decaying roots modulates litter decomposition through alterations in microbial functionality. Furthermore, Nuccio et al., 2020 specifically describe how both temporal and spatial niche microbial coexistence is fostered in the combined

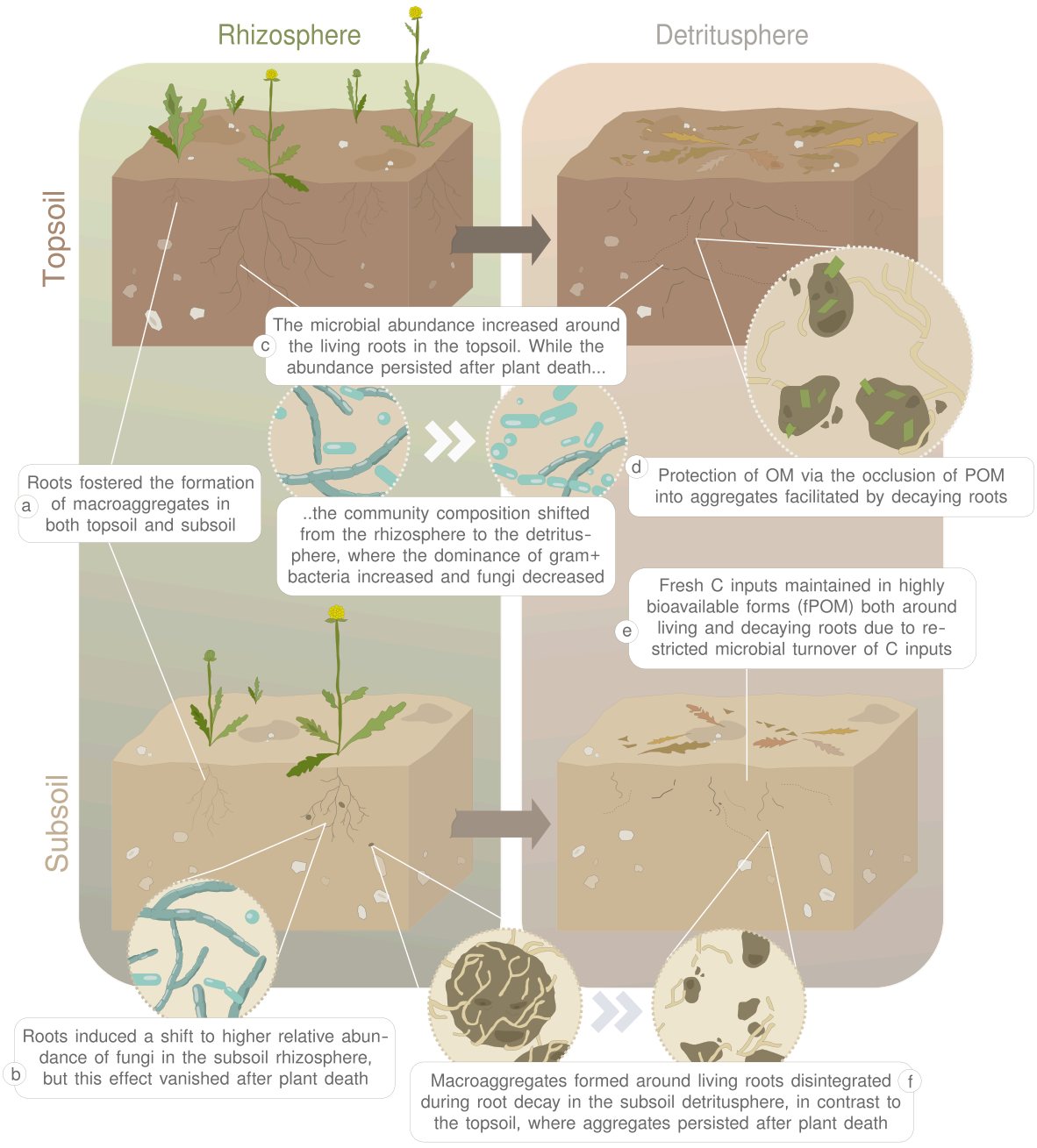

Fig. 4. **a** Living roots fostered the formation of macroaggregates in both topsoil and subsoil, and **b** induced a change in the microbial community composition in the subsoil towards a higher relative abundance of fungi. This was not reflected in the topsoil, where **c** the microbial abundance instead increased uniformly in the rhizosphere without structural changes in the community. While the increased total microbial abundance was maintained in the detritusphere, the composition changed as gram + bacteria outcompeted fungi. Around decaying roots in the topsoil, **d** OM was protected in aggregates via the formation of occluded POM ($oPOM_{<20\mu m}$) and in the subsoil, **e** the slower microbial C turnover resulted in an accumulation of fresh C inputs in highly bioavailable forms (fPOM) around both living and decaying roots. While the root-induced macroaggregates persisted after plant death in the topsoil, **f** the aggregates disintegrated in the subsoil around the decaying roots.

rhizosphere-detritusphere, which opens up important future research opportunities in the transition zone from rhizosphere to detritusphere and highlights need for further research including microbial functional traits.

Interestingly, the shift in the microbiome around decaying roots in the topsoil was not associated with a change in overall abundance—in fact, abundance prevailed from the rhizosphere to the detritusphere phase, while decreasing in the corresponding controls (Fig. 3 a). Consequently, despite the resource-limited conditions as decomposition progressed, litter-derived C inputs were sufficient to maintain microbial abundance, but the conditions favored those microbial groups specialized in utilizing complex C sources.

Another shift in microbial community structure in the detritusphere was observed in fungi, where both total fungal abundance and relative abundance to bacteria decreased, particularly so in the subsoil (Fig. 3 b and d). The shift towards bacterial dominance in the detritusphere contrasts with the general notion of fungi as key players in litter decomposition (Williams et al., 2006; Voříšková and Baldrian, 2013). As PLFA profiles were only quantified at one point during the decomposition process in the present study, this represents only a snapshot of the ongoing succession of the microbial community involved in decomposition. Herman et al. (2012) found that fungal dominance during litter

decomposition decreased rapidly after 21 days, after which gram+ and gram− increased. Voříšková and Baldrian (2013) further emphasized the succession of the fungal community during decomposition, with different fungal taxa being highly abundant only during short periods. Thus, our results do not necessarily exclude fungal involvement in the initial stages of litter decomposition, but rather point to the increasing importance of bacteria during the late stages of decomposition, when labile litter components are depleted. This is supported by Esperschütz et al. (2011) showing how gram + outcompete fungi in litter degradation in resource-limited systems where N is scarce. The retreat of fungi in the developed detritusphere in subsoil equates to the loss of the hyphal networks that enmeshed soil particles, which may cause the disintegration of aggregates around the decaying roots. This underlines the direct involvement of hyphae as a temporary binding agent in the rhizosphere that does not persist into the detritusphere (Six et al., 2004).

4.3. Elemental composition of rhizosphere and detritusphere

Contrary to our hypothesis, roots had no notable effects on total C and N contents in the bulk soil in the rhizosphere in either of the two soil substrates (Fig. S3). It is possible that root inputs to the system were minor in comparison with other soil C pools, or that the inputs were rapidly processed by the stimulated microbial activity in the vicinity of the roots. Given the enhanced microbial abundance and changed community composition around the roots (Fig. 3), the second option appeared to be more likely. Nevertheless, it should be noted that the entire, thoroughly rooted pot was considered as 'rhizosphere' in the present study. Indeed, there is no clear definition of the spatial extent of the rhizosphere or where the boundaries of the rhizosphere are, as it depends on the parameters studied (Kuzyakov and Razavi, 2019). However, most root-driven processes are concentrated in the immediate soil volume around the roots and diluted in the surrounding soil. For example, microbial abundance has been shown to be concentrated in the first 1–2 mm around the roots (Marschner et al., 2012), and rhizodeposits may have restricted dispersal potential from the immediate soil volume around the roots (Kuzyakov and Razavi, 2019). This means that certain root effects may have been overseen, or diluted, given the large soil volume representing the rhizosphere. Under these circumstances, ^{13}C labeling of the pioneer plants might have facilitated the quantification of small-scale elemental changes, thereby allowing a more detailed understanding of the fate of root-derived C in the soil, both in the rhizosphere and the subsequent detritusphere (Teixeira et al., 2024).

4.4. Changes in POM around living and decaying roots

Surprisingly, neither living nor decaying roots affected the composition of POM and MAOM, as evidenced by consistent C and N contents and comparable chemical compositions in all fractions (Fig. S6; Fig. S8; Table S3). In the topsoil, however, occluded C as $oPOM_{<20\mu m}$ and the contribution of this fraction to total C and N were clearly affected—albeit in contrasting ways between the rhizosphere and the detritusphere (Fig. 2). In the soil around the living root system, a slight decrease in occluded C was observed compared to the control, suggesting increased aggregate turnover around the roots (Wang et al., 2020). Root-induced breakdown of aggregates, combined with stimulated microbial activity around the roots resulting in an enhanced rhizosphere priming effect, could be contributing factors to the release and ultimate loss of bioavailable POM in the rhizosphere (Cheng, 2009). Around the decaying roots, the pattern was reversed, where instead an accumulation of occluded C ($oPOM_{<20\mu m}$) was determined (Fig. 4 d). This highlights decaying roots as a prerequisite for the formation of occluded POM and shows how decaying litter surfaces in the detritusphere represent functional components that facilitate aggregate formation, directly contributing to the long-term stabilization of organic C in the soil (Witzgall et al., 2021).

In the subsoil, we observed elevated C:N ratios in the fPOM fractions in both the rhizosphere and detritusphere compared to unplanted controls (Fig. S6; Fig. 4 e). During the rhizosphere phase, this was further associated with ^{15}N depletion, indicating fresh C inputs into the fraction, as the opposite—increasing aliphaticity of OM—would otherwise lead to ^{15}N accumulation (Fig. S7; Kramer et al., 2003). This means that fresh C inputs remained in highly bioavailable forms (*i.e.,* not occluded into aggregates or associated with mineral surfaces) and did not undergo notable microbial transformation during the course of both incubation phases. This phenomenon was only observed in subsoil, as there was no evidence of fresh C inputs in the fPOM fraction in the topsoil. This difference between the soil substrates can be attributed to restricted microbial abundance in the subsoil, resulting in slower C turnover compared to the topsoil where labile inputs were rapidly transformed. This may, in part, be related to the chemistry of the plant tissue in the subsoil, where roots were of lower biochemical quality compared to those in the topsoil (broader C:N ratios and elevated $lignin_{NMR}$:N ratios; Table 1; Walela et al., 2014). These findings highlight the limiting conditions for microbial activity and suggest that lower quality litter is less preferred as a nutrient source for microbial decomposers. Collectively, these observations underscore the importance of roots as a critical source of POM in dryland subsoils, with legacy effects that can persist even after plant death (Angst et al., 2016). Furthermore, they emphasize how the litter chemistry of OM inputs shapes microbial community composition, with implications for aggregate formation.

5. Conclusion

In this study, we explore the interaction between plant roots, microorganisms, and soil during the succession from a rhizosphere to a root detritusphere in a dryland topsoil and subsoil. Our results highlight the fundamental role of roots in driving soil structure formation, microbial succession, and OM formation during the early stages of soil development. While we found root-induced macroaggregation in the topsoil, the effect of roots was extended to both increased macro- and microaggregates in the subsoil, presumably facilitated by fungal hyphae in the subsoil rhizosphere. However, with plant death, as the rhizosphere transitioned to a detritusphere, the newly formed aggregates disintegrated in the subsoil, underscoring the critical importance of continuous OM inputs for maintaining more persistent aggregate structures in C-poor subsoils. The transition to a detritusphere was further associated with a clear decline in fungal abundance and an increased dominance of gram + bacteria, emphasizing their role in mineralizing increasingly complex C resources in the developing detritusphere in dryland soils. Conversely, we found legacy effects of living roots imprinted in the topsoil, as macroaggregates formed within the rhizosphere persisted after plant death, and the microbiome developed around living roots was maintained in the detritusphere. While we found no changes in MAOM around the roots, we highlight the build-up of occluded POM facilitated by decaying root litter in the topsoil, underscoring the influence of root residues on SOM formation and persistence within the root detritusphere. Our work thus highlights the intricate interactions of plants, microorganisms, and soil particles in the vicinity of living and decaying roots in dryland soil systems, and how the biogeochemical processes involved are regulated by the soil substrate in which the roots grow and decompose. Our results further underscore the importance of encompassing the *in situ* transition from living to decaying roots to advance our understanding of the dynamics of the legacy from rhizosphere and detritusphere.

CRediT authorship contribution statement

K. Witzgall: Writing – review & editing, Writing – original draft, Visualization, Methodology, Investigation, Formal analysis, Data curation, Conceptualization. **F.A. Steiner:** Writing – review & editing, Writing – original draft, Investigation, Formal analysis, Data curation, Conceptualization. **B.D. Hesse:** Writing – review & editing,

Investigation, Data curation. **N. Riveras-Muñoz:** Writing – review & editing, Methodology, Data curation. **V. Rodríguez:** Writing – review & editing, Methodology, Data curation. **P.P.C. Teixeira:** Writing – review & editing, Validation, Investigation. **M. Li:** Methodology. **R. Oses:** Writing – review & editing, Conceptualization. **O. Seguel:** Writing – review & editing, Conceptualization. **S. Seitz:** Writing – review & editing, Conceptualization. **D. Wagner:** Writing – review & editing, Supervision, Conceptualization. **T. Scholten:** Writing – review & editing, Supervision, Resources, Funding acquisition, Conceptualization. **F. Buegger:** Writing – review & editing, Formal analysis, Data curation. **G. Angst:** Writing – review & editing, Supervision, Data curation, Conceptualization. **C.W. Mueller:** Writing – review & editing, Validation, Supervision, Project administration, Methodology, Funding acquisition, Conceptualization.

Declaration of competing interest

The authors declare that they have no known competing financial interests or personal relationships that could influence the work reported in this paper.

Data availability

Data will be made available on request.

Acknowledgements

The authors are grateful for the help and support of Maria Greiner and Nina Meschnark who supported the laboratory analyses. We also thank Josef Reischenbeck who built the machine used for aggregate fractionation. This work was financially by the German Research Foundation (DFG) as part of the 'EarthShape' priority program [grant no. MU3021/6–2; www.earthshape.net].

Appendix A. Supplementary data

Supplementary data to this article can be found online at https://doi.org/10.1016/j.soilbio.2024.109503.

References

Albaladejo, J., Ortiz, R., Garcia-Franco, N., Navarro, A.R., Almagro, M., Pintado, J.G., Martínez-Mena, M., 2013. Land use and climate change impacts on soil organic carbon stocks in semi-arid Spain. Journal of Soils and Sediments 13, 265–277. https://doi.org/10.1007/s11368-012-0617-7.

Angst, G., Kögel-Knabner, I., Kirfel, K., Hertel, D., Mueller, C.W., 2016. Spatial distribution and chemical composition of soil organic matter fractions in rhizosphere and non-rhizosphere soil under European beech (Fagus sylvatica L.). Geoderma 264, 179–187. https://doi.org/10.1016/j.geoderma.2015.10.016.

Angst, G., Mueller, K.E., Kögel-Knabner, I., Freeman, K.H., Mueller, C.W., 2017. Aggregation controls the stability of lignin and lipids in clay-sized particulate and mineral associated organic matter. Biogeochemistry 132, 307–324. https://doi.org/10.1007/s10533-017-0304-2.

Angst, G., Messinger, J., Greiner, M., Häusler, W., Hertel, D., Kirfel, K., Kögel-Knabner, I., Leuschner, C., Rethemeyer, J., Mueller, C.W., 2018. Soil organic carbon stocks in topsoil and subsoil controlled by parent material, carbon input in the rhizosphere, and microbial-derived compounds. Soil Biology and Biochemistry 122, 19–30. https://doi.org/10.1016/j.soilbio.2018.03.026.

Baldock, J.A., Oades, J.M., Nelson, P.N., Skene, T.M., Golchin, A., Clarke, P., 1997. Assessing the extent of decomposition of natural organic materials using solid-state ^{13}C NMR spectroscopy. Soil Research 35 (5), 1061–1084. https://doi.org/10.1071/S97004.

Baumert, V.L., Vasilyeva, N.A., Vladimirov, A.A., Meier, I.C., Kögel-Knabner, I., Mueller, C.W., 2018. Root exudates induce soil macroaggregation facilitated by fungi in subsoil. Frontiers in Environmental Science 6. https://doi.org/10.3389/fenvs.2018.00140.

Baumert, V.L., Forstner, S.J., Zethof, J.H.T., Vogel, C., Heitkötter, J., Schulz, S., Kögel-Knabner, I., Mueller, C.W., 2021. Root-induced fungal growth triggers macroaggregation in forest subsoils. Soil Biology and Biochemistry 157, 108244. https://doi.org/10.1016/j.soilbio.2021.108244.

Berg, B., McClaugherty, C., 2008. Plant Litter: Decomposition, Humus Formation, Carbon Sequestration (No. 04; QH541. 5. S6, B4 2008. Springer, Berlin. https://doi.org/10.1007/978-3-642-38821-7.

Bernhard, N., Moskwa, L.M., Schmidt, K., Oeser, R.A., Aburto, F., Bader, M.Y., et al., 2018. Pedogenic and microbial interrelations to regional climate and local topography: new insights from a climate gradient (arid to humid) along the Coastal Cordillera of Chile. Catena 170, 335–355. https://doi.org/10.1016/j.catena.2018.06.018.

Brant, J.B., Myrold, D.D., Sulzman, E.W., 2006. Root controls on soil microbial community structure in forest soils. Oecologia 148, 650–659. https://doi.org/10.1007/s00442-006-0402-7.

Bonanomi, G., Incerti, G., Giannino, F., Mingo, A., Lanzotti, V., Mazzoleni, S., 2013. Litter quality assessed by solid state ^{13}C NMR spectroscopy predicts decay rate better than C/N and Lignin/N ratios. Soil Biology and Biochemistry 56, 40–48. https://doi.org/10.1016/j.soilbio.2012.03.003.

Bossuyt, H., Denef, K., Six, J., Frey, S.D., Merckx, R., Paustian, K., 2001. Influence of microbial populations and residue quality on aggregate stability. Applied Soil Ecology 16, 195–208. https://doi.org/10.1016/S0929-1393(00)00116-5.

Butler, J.L., Williams, M.A., Bottomley, P.J., Myrold, D.D., 2003. Microbial community dynamics associated with rhizosphere carbon flow. Applied and Environmental Microbiology 69 (11), 6793–6800. https://doi.org/10.1128/AEM.69.11.6793-6800.2003.

Bucka, F.B., Kölbl, A., Uteau, D., Peth, S., Kögel-Knabner, I., 2019. Organic matter input determines structure development and aggregate formation in artificial soils. Geoderma 354, 113881. https://doi.org/10.1016/j.geoderma.2019.113881.

Bucka, F.B., Felde, V.J., Peth, S., Kögel-Knabner, I., 2021. Disentangling the effects of OM quality and soil texture on microbially mediated structure formation in artificial model soils. Geoderma 403, 115213. https://doi.org/10.1016/j.geoderma.2021.115213.

Chabbi, A., Kögel-Knabner, I., Rumpel, C., 2009. Stabilised carbon in subsoil horizons is located in spatially distinct parts of the soil profile. Soil Biology and Biochemistry 41 (2), 256–261. https://doi.org/10.1016/j.soilbio.2008.10.033.

Chandler, D.G., Day, N., Madsen, M.D., Belnap, J., 2019. Amendments fail to hasten biocrust recovery or soil stability at a disturbed dryland sandy site. Restoration Ecology 27 (2), 289–297. https://doi.org/10.1111/rec.12870.

Cheng, W., 2009. Rhizosphere priming effect: its functional relationships with microbial turnover, evapotranspiration, and C–N budgets. Soil Biology and Biochemistry 41 (9), 1795–1801. https://doi.org/10.1016/j.soilbio.2008.04.018.

Chenu, C., Consentino, D.J., 2011. Microbial regulation of soil structural dynamics. In: Ritz, K., Young, I.M. (Eds.), The Architecture and Biology of Soils: Life in Inner Space (CABI, 2011). https://doi.org/10.1079/9781845935320.0037.

Costa, O.Y., Raaijmakers, J.M., Kuramae, E.E., 2018. Microbial extracellular polymeric substances: ecological function and impact on soil aggregation. Frontiers in Microbiology 9, 1636. https://doi.org/10.3389/fmicb.2018.01636.

Cotrufo, M.F., Soong, J.L., Horton, A.J., Campbell, E.E., Haddix, M.L., Wall, D.H., Parton, W.J., 2015. Formation of soil organic matter via biochemical and physical pathways of litter mass loss. Nature Geoscience 8 (10), 776–779. https://doi.org/10.1038/ngeo2520.

De Boer, W.D., Folman, L.B., Summerbell, R.C., Boddy, L., 2005. Living in a fungal world: impact of fungi on soil bacterial niche development. FEMS Microbiology Reviews 29 (4), 795–811. https://doi.org/10.1016/j.femsre.2004.11.005.

Denef, K., Six, J., Merckx, R., Paustian, K., 2002. Short-term effects of biological and physical forces on aggregate formation in soils with different clay mineralogy. Plant and Soil 246, 185–200. https://doi.org/10.1023/A:1020668013524.

Denef, K., Roobroeck, D., Manimel Wadu, M.C.W., Lootens, P., Boeckx, P., 2009. Microbial community composition and rhizodeposit-carbon assimilation in differently managed temperate grassland soils. Soil Biology and Biochemistry 41 (1), 144–153. https://doi.org/10.1016/j.soilbio.2008.10.008.

Dhillion, S.S., Vidiella, P.E., Aquilera, L.E., Friese, C.F., De Leon, E., Armesto, J.J., Zak, J. C., 1995. Mycorrhizal plants and fungi in the fog-free Pacific coastal desert of Chile. Mycorrhiza 5, 381–386. https://doi.org/10.1007/BF00207410.

Esperschütz, J., Welzl, G., Schreiner, K., Buegger, F., Munch, J.C., Schloter, M., 2011. Incorporation of carbon from decomposing litter of two pioneer plant species into microbial communities of the detritusphere. FEMS Microbiology Letters 320 (1), 48–55. https://doi.org/10.1111/j.1574-6968.2011.02286.x.

Eusterhues, K., Rumpel, C., Kleber, M., Kögel-Knabner, I., 2003. Stabilisation of soil organic matter by interactions with minerals as revealed by mineral dissolution and oxidative degradation. Organic Geochemistry 34 (12), 1591–1600. https://doi.org/10.1016/j.orggeochem.2003.08.007.

Fanin, N., Kardol, P., Farrell, M., Nilsson, M.C., Gundale, M.J., Wardle, D.A., 2019. The ratio of Gram-positive to Gram-negative bacterial PLFA markers as an indicator of carbon availability in organic soils. Soil Biology and Biochemistry 128, 111–114. https://doi.org/10.1016/j.soilbio.2018.10.010.

Felde, V.J., Schweizer, S.A., Biesgen, D., Ulbrich, A., Uteau, D., Knief, C., Graf-Rosenfellner, M., Kögel-Knabner, I., Peth, S., 2020. Wet sieving versus dry crushing: soil microaggregates reveal different physical structure, bacterial diversity and organic matter composition in a clay gradient. European Journal of Soil Science 72 (2), 810–828. https://doi.org/10.1111/ejss.13014.

Frostegård, Å., Bååth, E., Tunlio, A., 1993. Shifts in the structure of soil microbial communities in limed forests as revealed by phospholipid fatty acid analysis. Soil Biology and Biochemistry 25 (6), 723–730. https://doi.org/10.1016/0038-0717(93)90113-P.

Gregory, P.J., 2022. RUSSELL REVIEW Are plant roots only "in" soil or are they "of" it? Roots, soil formation and function. European Journal of Soil Science 73 (1), e13219. https://doi.org/10.1111/ejss.13219.

Golchin, A., Baldock, J., Oades, J., 1997. A model linking organic matter decomposition. Chemistry, and Aggregate Dynamics. Soil Processes and the Carbon Cycle. CRC Press, Boca Raton, pp. 245–266. https://doi.org/10.1201/9780203739273.

Helfrich, M., Ludwig, B., Potthoff, M., Flessa, H., 2008. Effect of litter quality and soil fungi on macroaggregate dynamics and associated partitioning of litter carbon and nitrogen. Soil Biology and Biochemistry 40 (7), 1823–1835. https://doi.org/10.1016/j.soilbio.2008.03.006.

Herman, D.J., Firestone, M.K., Nuccio, E., Hodge, A., 2012. Interactions between an arbuscular mycorrhizal fungus and a soil microbial community mediating litter decomposition. FEMS Microbiology Ecology 80 (1), 236–247. https://doi.org/10.1111/j.1574-6941.2011.01292.x.

Hinsinger, P., Bengough, A.G., Vetterlein, D., Young, I.M., 2009. Plant-microbe-soil interactions in the rhizosphere: an evolutionary perspective. Plant and Soil 321, 83–115. https://doi.org/10.1007/s11104-009-0042-x, 2009.

IUSS Working Group WRB, 2015. World reference base for soil resources 2014, Update 2015. International soil classification system for naming soils and creating legends for soil maps. World Soil Resources Report No. 106. FAO. https://www.fao.org/3/i3794en/I3794en.pdf.

Jobbágy, E.G., Jackson, R.B., 2001. The distribution of soil nutrients with depth: global patterns and the imprint of plants. Biogeochemistry 53, 51–77. https://doi.org/10.1016/S0065-2113(05)88002-2.

Jones, D.L., Nguyen, C., Finlay, R.D., 2009. Carbon flow in the rhizosphere: carbon trading at the soil–root interface. Plant and Soil 321, 5–33. https://doi.org/10.1016/j.soilbio.2008.10.034.

Kopittke, P.M., Dalal, R.C., Hoeschen, C., Li, C., Menzies, N.W., Mueller, C.W., 2020. Soil organic matter is stabilized by organo-mineral associations through two key processes: the role of the carbon to nitrogen ratio. Geoderma 357, 113974. https://doi.org/10.1016/j.geoderma.2019.113974.

Kramer, M.G., Sollins, P., Sletten, R.S., Swart, P.K., 2003. N isotope fractionation and measures of organic matter alteration during decomposition. Ecology 84 (8), 2021–2025.

Kramer, S., Marhan, S., Haslwimmer, H., Ruess, L., Kandeler, E., 2013. Temporal variation in surface and subsoil abundance and function of the soil microbial community in an arable soil. Soil Biology and Biochemistry 61, 76–85. https://doi.org/10.1016/j.soilbio.2013.02.006.

Kravchenko, A.N., Guber, A.K., 2017. Soil pores and their contributions to soil carbon processes. Geoderma 287, 31–39. https://doi.org/10.1016/j.geoderma.2016.06.027.

Kuzyakov, Y., Razavi, B.S., 2019. Rhizosphere size and shape: temporal dynamics and spatial stationarity. Soil Biology and Biochemistry 135, 343–360. https://doi.org/10.1016/j.soilbio.2019.05.011.

Kögel-Knabner, I., Zech, W., Hatcher, P.G., 1988. Chemical composition of the organic matter in forest soils: the humus layer. Zeitschrift für Pflanzenernährung und Bodenkunde 151, 331–340. https://doi.org/10.1002/jpln.19881510512.

Lal, R., 2020. Soil organic matter and water retention. Agronomy Journal 112 (5), 3265–3277. https://doi.org/10.1002/agj2.20282.

Lehmann, A., Zheng, W., Ryo, M., Soutschek, K., Roy, J., Rongstock, R., Maaß, S., Rillig, M.C., 2020. Fungal traits important for soil aggregation. Frontiers in Microbiology 10, 2904. https://doi.org/10.3389/fmicb.2019.02904.

Luebert, F., Pliscoff, P., 2006. Sinopsis bioclimática y vegetacional de Chile. Editorial Universitaria, Santiago de Chile.

Marschner, P., Marhan, S., Kandeler, E., 2012. Microscale distribution and function of soil microorganisms in the interface between rhizosphere and detritusphere. Soil Biology and Biochemistry 49, 174–183. https://doi.org/10.1016/j.soilbio.2012.01.033.

Ministerio de Obras Públicas, M., 2017. Información Oficial Hidrometeorológica y de Calidad de Aguas en Línea. In: DGA.

Mueller, C.W., Koegel-Knabner, I., 2009. Soil organic carbon stocks, distribution, and composition affected by historic land use changes on adjacent sites. Biology and Fertility of Soils 45 (4), 347–359. https://doi.org/10.1007/s00374-008-0336-9.

Murphy, B.W., 2015. Impact of soil organic matter on soil properties—a review with emphasis on Australian soils. Soil Research 53 (6), 605–635. https://doi.org/10.1071/SR14246.

Nelson, P.N., Baldock, J.A., 2005. Estimating the molecular composition of a diverse range of natural organic materials from solid-state ^{13}C NMR and elemental analyses. Biogeochemistry 72, 1–34. https://doi.org/10.1007/s10533-004-0076-3.

Nuccio, E.E., Starr, E., Karaoz, U., Brodie, E.L., Zhou, J., Tringe, S.G., Malmstrom, R.R., Woyke, T., Banfield, J.F., Firestone, M.K., Pett-Ridge, J., 2020. Niche differentiation is spatially and temporally regulated in the rhizosphere. The ISME journal 14 (4), 999–1014. https://doi.org/10.1038/s41396-019-0582-x.

Oeser, R.A., Stroncik, N., Moskwa, L.M., Bernhard, N., Schaller, M., Canessa, R., et al., 2018. Chemistry and microbiology of the Critical Zone along a steep climate and vegetation gradient in the Chilean Coastal Cordillera. Catena 170, 183–203. https://doi.org/10.1016/j.catena.2018.06.002.

O'Leary, W.M., Wilkinson, S.G., 1988. Gram-positive bacteria. In: Ratledge, C., Wilkinson, S.G. (Eds.), Microbial Lipids, vol. 1. Academic Press, London, pp. 117–201.

Oliver, I.C., Knox, O.G., Flavel, R.J., Wilson, B.R., 2021. Rhizosphere legacy: plant root interactions with the soil and its biome. Rhizosphere Biology: Interactions Between Microbes and Plants 129–153. https://doi.org/10.1007/978-981-15-6125-2_6.

Peixoto, L., Elsgaard, L., Rasmussen, J., Kuzyakov, Y., Banfield, C.C., Dippold, M.A., Olesen, J.E., 2020. Decreased rhizodeposition, but increased microbial carbon stabilization with soil depth down to 3.6 m. Soil Biology and Biochemistry 150, 108008. https://doi.org/10.1016/j.soilbio.2020.108008.

Phillips, R.L., Zak, D.R., Holmes, W.E., White, D.C., 2002. Microbial community composition and function beneath temperate trees exposed to elevated atmospheric carbon dioxide and ozone. Oecologia 131, 236–244. https://doi.org/10.1007/s00442-002-0868-x.

Poll, C., Ingwersen, J., Stemmer, M., Gerzabek, M.H., Kandeler, E., 2006. Mechanisms of solute transport affect small-scale abundance and function of soil microorganisms in the detritusphere. European Journal of Soil Science 57 (4), 583–595. https://doi.org/10.1111/j.1365-2389.2006.00835.x.

Poll, C., Marhan, S., Ingwersen, J., Kandeler, E., 2008. Dynamics of litter carbon turnover and microbial abundance in a rye detritusphere. Soil Biology and Biochemistry 40 (6), 1306–1321. https://doi.org/10.1016/j.soilbio.2007.04.002.

Poll, C., Brune, T., Begerow, D., Kandeler, E., 2010. Small-scale diversity and succession of fungi in the detritusphere of rye residues. Microbial Ecology 59, 130–140. https://doi.org/10.1007/s00248-009-9541-9.

Prater, I., Zubrzycki, S., Buegger, F., Zoor-Füllgraff, L.C., Angst, G., Dannenmann, M., Mueller, C.W., 2020. From fibrous plant residues to mineral-associated organic carbon–the fate of organic matter in Arctic permafrost soils. Biogeosciences 17 (13), 3367–3383. https://doi.org/10.5194/bg-17-3367-2020.

Rasse, D.P., Rumpel, C., Dignac, M.F., 2005. Is soil carbon mostly root carbon? Mechanisms for a specific stabilisation. Plant and Soil 269 (1–2), 341–356. https://doi.org/10.1007/s11104-004-0907-y.

R Development Core Team, 2008. In: R: A Language and Environment for Statistical Computing. http://www.R-project.org.

RStudio Team, 2015. In: RStudio: Integrated Development for R. http://www.rstudio.com/.

Richter, D.D.B., Oh, N.H., Fimmen, R., Jackson, J., 2007. The rhizosphere and soil formation. In: The Rhizosphere (Pp. 179-IN2). Academic Press. https://doi.org/10.1016/B978-012088775-0/50010-0.

Rillig, M.C., Mummey, D.L., 2006. Mycorrhizas and soil structure. New Phytologist 171 (1), 41–53. https://doi.org/10.1111/j.1469-8137.2006.01750.x.

Riveras-Muñoz, N., Seitz, S., Witzgall, K., Rodríguez, V., Kühn, P., Mueller, C.W., Oses, R., Seguel, O., Wagner, D., Scholten, T., 2022. Biocrust-linked changes in soil aggregate stability along a climatic gradient in the Chilean Coastal Range. Soils 8 (2), 717–731. https://doi.org/10.5194/soil-8-717-2022.

Rötzer, M., Prechtel, A., Ray, N., 2023. Pore scale modeling of the mutual influence of roots and soil aggregation in the rhizosphere. Frontiers in Soil Science 3. https://doi.org/10.3389/fsoil.2023.1155889.

Scholes, R.J., 2020. The future of semi-arid regions: a weak fabric unravels. Climate 8 (3), 43. https://doi.org/10.3390/cli8030043.

Shi, S., Herman, D.J., He, Z., Pett-Ridge, J., Wu, L., Zhou, J., Firestone, M.K., 2018. Plant roots alter microbial functional genes supporting root litter decomposition. Soil Biology and Biochemistry 127, 90–99. https://doi.org/10.1016/j.soilbio.2018.09.013.

Six, J., Bossuyt, H., Degryze, S., Denef, K., 2004. A history of research on the link between (micro) aggregates, soil biota, and soil organic matter dynamics. Soil and Tillage Research 79 (1), 7–31. https://doi.org/10.1016/j.still.2004.03.008.

Sokol, N.W., Sanderman, J., Bradford, M.A., 2019. Pathways of mineral-associated soil organic matter formation: integrating the role of plant carbon source, chemistry, and point of entry. Global Change Biology 25 (1), 12–24. https://doi.org/10.1111/gcb.14482.

Teixeira, P.P., Vidal, A., Teixeira, A.P.M., Souza, I.F., Hurtarte, L.C.C., Silva, D.H., Silva, D.H.S., Almeida, L.F.J., Buegger, F., Hammer, E.C., Jansa, J., Mueller, C.W., Silva, I.R., 2024. Decoding the rhizodeposit-derived carbon's journey into soil organic matter. Geoderma 443, 116811. https://doi.org/10.1016/j.geoderma.2024.116811.

Theuerl, S., Buscot, F., 2010. Laccases: toward disentangling their diversity and functions in relation to soil organic matter cycling. Biology and Fertility of Soils 46, 215–225. https://doi.org/10.1007/s00374-010-0440-5.

Tian, J., Dippold, M., Pausch, J., Blagodatskaya, E., Fan, M., Li, X., Kuzyakov, Y., 2013. Microbial response to rhizodeposition depending on water regimes in paddy soils. Soil Biology and Biochemistry 65, 195–203. https://doi.org/10.1016/j.soilbio.2013.05.021.

Tisdall, J.M., Oades, J.M., 1982. Organic matter and water-stable aggregates in soils. Journal of Soil Science 33 (2), 141–163. https://doi.org/10.1111/j.1365-2389.1982.tb01755.x.

Uroz, S., Calvaruso, C., Turpault, M.P., Frey-Klett, P., 2009. Mineral weathering by bacteria: ecology, actors and mechanisms. Trends in Microbiology 17 (8), 378–387. https://doi.org/10.1016/j.tim.2009.05.004.

Vidal, A., Hirte, J., Bender, S.F., Mayer, J., Gattinger, A., Höschen, C., Schädler, S., Iqbal, T.M., Mueller, C.W., 2018. Linking 3D soil structure and plant-microbe-soil carbon transfer in the rhizosphere. Frontiers in Environmental Science 6, 9. https://doi.org/10.3389/fenvs.2018.00009.

Vidal, A., Klöffel, T., Guigue, J., Angst, G., Steffens, M., Hoeschen, C., Mueller, C.W., 2021. Visualizing the transfer of organic matter from decaying plant residues to soil mineral surfaces controlled by microorganisms. Soil Biology and Biochemistry 160, 108347. https://doi.org/10.1016/j.soilbio.2021.108347.

Villarino, S.H., Pinto, P., Jackson, R.B., Piñeiro, G., 2021. Plant rhizodeposition: a key factor for soil organic matter formation in stable fractions. Science Advances 7 (16), eabd3176. https://doi.org/10.1126/sciadv.abd3176.

Voříšková, J., Baldrian, P., 2013. Fungal community on decomposing leaf litter undergoes rapid successional changes. The ISME journal 7 (3), 477–486. https://doi.org/10.1038/ismej.2012.116.

Walela, C., Daniel, H., Wilson, B., Lockwood, P., Cowie, A., Harden, S., 2014. The initial lignin: nitrogen ratio of litter from above and below ground sources strongly and negatively influenced decay rates of slowly decomposing litter carbon pools. Soil Biology and Biochemistry 77, 268–275. https://doi.org/10.1016/j.soilbio.2014.06.013.

Wang, Q., Wang, Y., Wang, S., He, T., Liu, L., 2014. Fresh carbon and nitrogen inputs alter organic carbon mineralization and microbial community in forest deep soil

layers. Soil Biology and Biochemistry 72, 145–151. https://doi.org/10.1016/j.soilbio.2014.01.020.

Wang, X., Yin, L., Dijkstra, F.A., Lu, J., Wang, P., Cheng, W., 2020. Rhizosphere priming is tightly associated with root-driven aggregate turnover. Soil Biology and Biochemistry 149, 107964. https://doi.org/10.1016/j.soilbio.2020.107964.

Weber, B., Belnap, J., Büdel, B., Antoninka, A.J., Barger, N.N., Chaudhary, V.B., Bowker, M.A., 2022. What is a biocrust? A refined, contemporary definition for a broadening research community. Biological Reviews 97 (5), 1768–1785. https://doi.org/10.1111/brv.12862.

Williams, M.A., Myrold, D.D., Bottomley, P.J., 2006. Carbon flow from ^{13}C-labeled straw and root residues into the phospholipid fatty acids of a soil microbial community under field conditions. Soil Biology and Biochemistry 38 (4), 759–768. https://doi.org/10.1016/j.soilbio.2005.07.001.

Witzgall, K., Vidal, A., Schubert, D.I., Höschen, C., Schweizer, S.A., Buegger, F., Pouteau, V., Chenu, C., Mueller, C.W., 2021. Particulate organic matter as a functional soil component for persistent soil organic carbon. Nature Communications 12 (1), 4115. https://doi.org/10.1038/s41467-021-24192-8.

Wurst, S., Ohgushi, T., 2015. Do plant-and soil-mediated legacy effects impact future biotic interactions? Functional Ecology 29 (11), 1373–1382. https://doi.org/10.1111/1365-2435.12456.